ORIGINAL ARTICLE

Adaptation of electrodes and printable gel polymer electrolytes for optimized fully organic batteries

Simon Muench[1,2] ⬤ | René Burges[1,2] | Alexandra Lex-Balducci[1,2] |
Johannes C. Brendel[1,2] | Michael Jäger[1,2] | Christian Friebe[1,2] |
Andreas Wild[3] | Ulrich S. Schubert[1,2] ⬤

[1]Laboratory of Organic and
Macromolecular Chemistry, Friedrich
Schiller University Jena, Jena, Germany

[2]Center for Energy and Environmental
Chemistry Jena, Friedrich Schiller
University Jena, Jena, Germany

[3]Research, Development & Innovation,
Evonik Operations GmbH, Marl,
Germany

Correspondence
Ulrich S. Schubert, Laboratory of Organic
and Macromolecular Chemistry, Friedrich
Schiller University Jena, Humboldtstr.10,
Jena 07743, Germany.
Email: ulrich.schubert@uni-jena.de

Funding information
Deutsche Forschungsgemeinschaft, Grant/
Award Number: 358263073; European
Regional Development Fund; Thüringer
Aufbaubank, Grant/Award Number:
2017FGR0055; Thüringer Ministerium für
Wirtschaft, Wissenschaft und Digitale
Gesellschaft; Emmy-Noether Programme,
Grant/Award Number: 358263073;
German Science Foundation; Evonik
Industries AG

Abstract

Despite intensive scientific efforts on the development of organic batteries, their
full potential is still not being realized. The individual components, such as elec-
trode materials and electrolytes, are in most cases developed independently and
are not adjusted to each other. In this context, we report on the performance opti-
mization of a full-organic solid-state battery system by the mutual adaptation of
the electrode materials and an ionic liquid (IL)-based gel polymer electrolyte
(GPE). The formulation of the latter was designed for a one-step manufacturing
approach and can be applied directly to the electrode surface, where it is UV-
cured to yield the GPE without further post-treatment steps. Herein, a special
focus was placed on the applicability in industrial processes. A first significant
capacity increase was achieved by the incorporation of the IL into the electrode
composite. Furthermore, the GPE composition was adapted applying acrylate-
and methacrylate-based monomers and combinations thereof with the premise
of a fast curing step. Furthermore, the amount of IL was varied, and all combina-
tions were evaluated for their final performance in cells. The latter variation rev-
ealed that a high ionic conductivity is not the only determining factor for a good
cell performance. Next to a sufficient conductivity, the interaction between elec-
trode and electrolyte plays a key role for the cell performance as it enhances the
accessibility of the counter ions to the redox-active sites.

KEYWORDS

electrode, energy storage, gel polymer electrolytes, organic battery, photo-polymerization,
polymeric material, redox-active material, solid state battery

1 | INTRODUCTION

New developments in the field of energy storage repre-
sent a significant topic in current research. Mobile
devices are becoming increasingly ubiquitous in our daily
life and demand for batteries with high energy densities
and long cycle lives at low costs.[1] Furthermore, stationary
energy storage represents a key component for the transi-
tion from fossil fuels to renewable energy sources in the
ongoing energy transfer.[2–3] Besides the development of

classical metal-based batteries, organic batteries became a major subject of recent battery research.[4–6] They feature several advantages compared to common metal-based batteries: They do not contain any toxic and rare heavy metals, their organic raw materials can potentially be obtained from renewable resources, and at the end of the life cycle they can be disposed by incineration without toxic leftovers. Furthermore, they enable a customizable design of mechanically flexible devices and can be produced in large quantities, due to the possible application of cheap mass-manufacturing techniques like roll-to-roll processing or various printing techniques. While organic active electrode materials were studied with rising interest over the last years, only a few studies were published that focus on electrolytes specifically designed for the use with organic electrode materials.[7-14] However, it is not only the electrochemical performance that can benefit from the mutual adjustment of electrodes and electrolytes. The development of a printable gel polymer electrolyte (GPE) system for organic electrode materials also enables the production of fully organic battery systems using printing techniques, paving the way for the mass production of low-cost battery systems.

In our recent study, we presented a GPE consisting of a methacrylate-based polymer matrix and an ionic liquid (IL) that provides the ionic conductivity.[15] It was designed to be printed directly on the electrode as a viscous paste that includes all components of the GPE and subsequently cured by UV-polymerization within a few minutes. The GPE provided a high ionic conductivity in the range of 10^{-4} S/cm at room temperature and sufficient mechanical stability to substitute the separator. Consequently, it was applied in all-organic batteries with a poly(2,2,6,6-tetramethyl-4-piperidinyl-N-oxyl methacrylate) (PTMA) cathode and a poly(2-vinyl-11,11,12,12-tetracyano-9,10-anthraquinonedimethane) anode, which revealed fast charging ability and high cycling stability.

This new material technology for printable batteries was presented for the first time in March 2019 by Evonik, under the brand name TAeTTOOz®.[16–17] In May 2020 Evonik presented their first technology demonstrator for printed electronics together with a development partner.[18]

In this consecutive study, we present the further development of the concept of printable organic battery materials. Electrode and electrolyte were adjusted to optimize their interaction and to improve the activity of the electrode material. For this purpose, the IL was integrated into the electrode composite and the GPE composition was varied regarding the type and ratio of the monomers as well as the amount of containing IL. With these optimizations, special emphasis was placed on the further reduction of the polymerization time to the range of 1 min and below to meet the requirements of real-life mass manufacturing.

2 | MATERIALS AND METHODS

A description of the materials and the equipment, as well as a table with detailed film compositions can be found in the supporting information S1. The impedance spectroscopy and the coin cell manufacturing were conducted as previously published.[15]

2.1 | General procedure for GPE manufacturing

The GPE manufacturing was carried out based on the procedure reported in our recent publication:[15] The monomers benzyl acrylate (Bn-A), benzyl methacrylate (Bn-MA), poly(ethylene glycol) methylether acrylate (mPEG-A, M_n: 480 g/mol), and poly(ethylene glycol) methylether methacrylate (mPEG-MA, M_n: 500 g/mol) were mixed in varying molar ratios (Table 1), whereas the molar ratio of benzyl (Bn) to poly(ethylene glycol) (mPEG) groups was kept at 3/1. Depending on the polymerizable group of the monomers, two different cross-linkers were investigated. 15 mol% of triethylene glycol dimethacrylate (TEG-DMA) and 5 mol% of poly(ethylene glycol) diacrylate (PEG-DA, M_n: 250 g/mol) (regarding to all monomers) were used for pure MA-based GPEs and for all mixtures containing acrylates, respectively. The amount of the IL 1-ethyl-3-methylimidazolium bis(trifluoromethyl sulfonyl)imide (EMImTFSI) was calculated from the combined volumes of the monomers and the cross-linker. This mixture was subsequently combined with the initiator Ivocerin® (0.5 mol% based on the monomers and the cross-linker) as well as fumed silica (5 wt% based on all components) and mixed by vigorous stirring with a spatula for 5 min. The paste was sealed in a vial with septum and vacuum (10^{-1} mbar) was applied. The vial was ultra-sonicated and refilled with argon. For the preparation of free-standing films for kinetic and impedance studies, the electrolyte formulation was placed between two siliconized PET-foils (PPI Adhesive Products GmbH). The film thickness of the resulting GPE was adjusted with a spacer to 400 μm. Residual material was pressed out of the pattern and the samples were placed into a UV chamber. For the preparation of GPEs directly polymerized on composite electrodes, the electrolyte formulation was applied via doctor blading onto the electrodes, which were fixed on a vacuum table (electrode thickness: 41–45 μm; blade gap: 500 μm; resulting GPE thickness: 330–380 μm), and subsequently irradiated with UV light (UV cube, Dr. Hönle AG). All samples were prepared under reduced light conditions (a filter foil for light of low wavelength was applied to the indirect lighting source) to avoid unwanted initiation.

TABLE 1 Overview of investigated GPE compositions

|	A/MA (mol/mol)	IL/M (vol/vol)	Cross-linker
1	0/100	2/1	15 mol% TEG-DMA
2	100/0	2/1	5 mol% PEG-DA
3	90/10	2/1	5 mol% PEG-DA
4	75/25	2/1	5 mol% PEG-DA
5	50/50	2/1	5 mol% PEG-DA
6	90/10	1/1	5 mol% PEG-DA
7	90/10	1/2	5 mol% PEG-DA
8	90/10	1/4	5 mol% PEG-DA

Abbreviations: GPE, gel polymer electrolyte; PEG-DA, poly(ethylene glycol) diacrylate; TEG-DMA, triethylene glycol dimethacrylate.

For the determination of the polymerization kinetics, the monomer conversions were investigated by ^{1}H NMR spectroscopy (Bruker AC 300) using EMImTFSI as internal standard (Figure S1). The insoluble cross-linked GPE samples were stirred overnight in DMSO-d$_6$ to dissolve the remaining not polymerized monomers and subsequently filtered through a syringe filter (PTFE, pore size 0.45 µm). The conversions were calculated from the ratios of the monomer double bond signals of the irradiated samples and the unpolymerized mixture. Exemplary ^{1}H NMR spectrum data of formulation 3 before UV radiation (300 MHz, DMSO-d$_6$, δ in ppm): EMImTFSI: 9.10 (s, 1H); 7.75 (m, 1H); 7.67 (m, 1H); 4.19 (q, 2H); 3.84 (s, 3H); 1.42 (t, 3H); monomers: 7.25–7.45 (m, Ar); 6.3 to 6.45 ppm (m, A sp^2); 6.1 to 6.3 ppm (m, A sp^2); 6.0–6.1 (m, MA sp^2); 5.9 to 6.0 ppm (m, A sp^2); 5.65–5.75 (m, MA sp^2); 5.18 (s, Bn); 3.4–3.7 (m, PEG); 3.23 (s, methoxy); 1.85–1.95 (m, MA sp^3).

3 | RESULTS AND DISCUSSION

3.1 | Electrode optimization

To investigate the electrochemical performance of the GPEs, an all-organic battery setup with PTMA cathodes and poly(imide) (PI) anodes was chosen (Scheme 1). PTMA is considered as one of the most promising cathode materials due to the robust redox reactions and high rate capabilities, while PI benefits from a multi-electron reduction and straightforward synthesis, which facilitates an industrial application, in particular compared to the anode material applied in our previous study.[19–21] For a better comparability of the results, the anode was oversized and all determined specific capacities refer to the mass of the active polymer in the
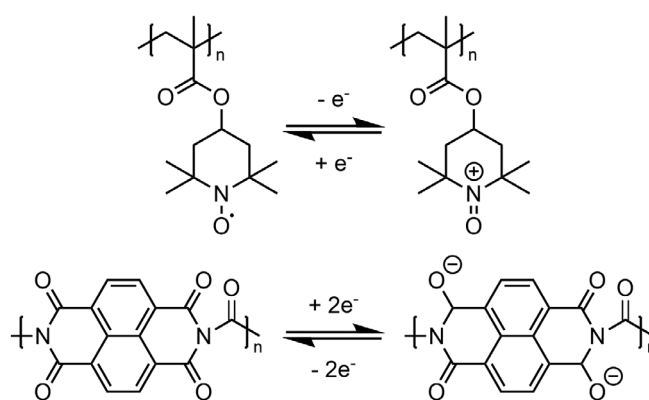
SCHEME 1 Schematic representation of the applied active polymers PTMA and poly(imide) (PI) and their utilized redox reactions

capacity-limiting cathode. In all galvanostatic cycling experiments, the cells were charged and discharged between 0.7 and 1.7 V at rates from 0.1C to 5C for 250 cycles in total.

Initially, cells were tested with neat liquid EMImTFSI as electrolyte, which was soaked in a Whatman® glass fiber separator. These cells, however, suffered from low specific capacities. In order to facilitate the accessibility of the redox-active sites at the polymers for the counter ions of EMImTFSI, the IL was also integrated into the electrode composite. This approach proved to be successful as the cell using electrodes with integrated IL showed a significant capacity increase (Figure 1). While electrodes without integrated EMImTFSI revealed a maximum capacity of 12 mAh/g at 0.1C, those with integrated IL showed 49 mAh/g. This provides a first indication that the interaction of the electrolyte counter ions with the active material represents a key factor to improve performance, even if the neat IL is applied as electrolyte without gelation in a polymer matrix.

3.2 | Influence of the monomer composition on the GPE performance

As next step the composition of the GPE was optimized. One important criterion for the mass production of printed organic batteries is a fast film formation of the GPE upon UV irradiation, which should be in the range of a few seconds. Therefore, the monomer combination was varied based on the previous GPE composition to ensure a fast polymerization while considering the influence on the cell performance.[15] The previously developed GPE consists of a cross-linked methacrylate-based polymer matrix with two different side groups: First, Bn groups to improve the mechanical properties and second, mPEG side chains for flexibility (Scheme 2). A ratio of Bn/mPEG of 3/1 (mol/mol) was chosen to ensure both sufficient mechanical stability and a high flexibility. An IL was chosen as supporting electrolyte, because it provides the required ionic species and acts as solvent/plasticizer, while it contains no scarce metal ions and is non-
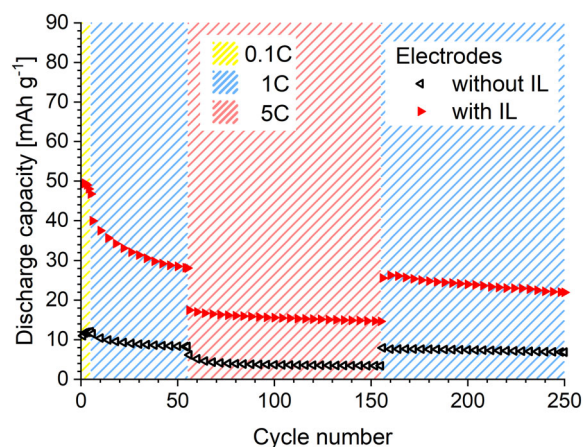

FIGURE 1 Discharge capacities derived from galvanostatic charge/discharge experiments of coin cells with PTMA cathode and poly(imide) (PI) anode (5 cycles at 0.1C, 50 cycles at 1C, 100 cycles at 5C, 95 cycles at 1C) for comparison of electrodes with and without EMImTFSI integrated into the composite with pristine ionic liquid (IL) as electrolyte. For clarity, only every fifth cycle is shown for the 1C and 5C rates [Color figure can be viewed at wileyonlinelibrary.com]
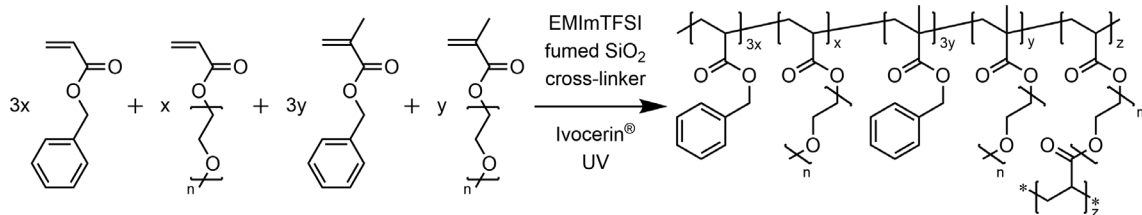
volatile, which is beneficial for the safety. To maintain a high conductivity, a ratio of the IL EMImTFSI to the monomer mixture (M) of 2/1 (vol/vol) was used. The viscosity of the formulation was adjusted by addition of a fumed silica nanofiller, which also have been reported to have a positive effect on the ionic conductivity.[22–25] As shown by indentation experiments in our previous work, this formulation resulted in a mechanically stable, flexible film after an irradiation time of 10 min when utilizing a combination of camphorquinone and p-dimethylamino ethylbenzoate as photo-initiator and 10 mol% TEG-DMA as cross-linker.[15]

Acrylate monomers (A) were considered in this work to reduce the polymerization time, as these monomers feature significantly higher polymerization rates compared to methacrylates (MA). *Bis*-4-methoxybenzoyl diethyl germanium (Ivocerin®) was used as initiator. As expected, the polymerization kinetics investigations (Figure 2(A)) revealed that the conversion of only 64% after 1 min UV irradiation for a MA-based formulation (1) increases to 98% for an A-based mixture (2). A high conversion is not only of interest for the mechanical properties of the GPE but also for the electrochemical performance of the cell, which can be negatively affected by residual monomers. In addition, the amount of cross-linker necessary for the formation of a mechanically stable film could be reduced from 15 mol% for MA-based formulations to 5 mol% for A-based mixtures.

However, in former works it was observed that MAs are beneficial regarding the electrochemical cell performance of full organic batteries.[26] Consequently, formulations of As with MAs as co-monomers were investigated. The amount of MA was varied from 10 to 50 mol% (Figure 2(B)). As expected, the polymerization rate decreases with increasing MA content with the MA monomers being consumed faster than the A monomers. This effect can be explained by the copolymerization parameters of As and MAs, which facilitate the integration of the latter.[27–28] Formulations with up to 25 mol% MA (compositions 3 and 4) reveal suitable polymerization times, reaching conversions of more than 90% for both MAs and As after 60 s. Thermogravimetric analysis (TGA, Figure S2) and differential scanning calorimetry
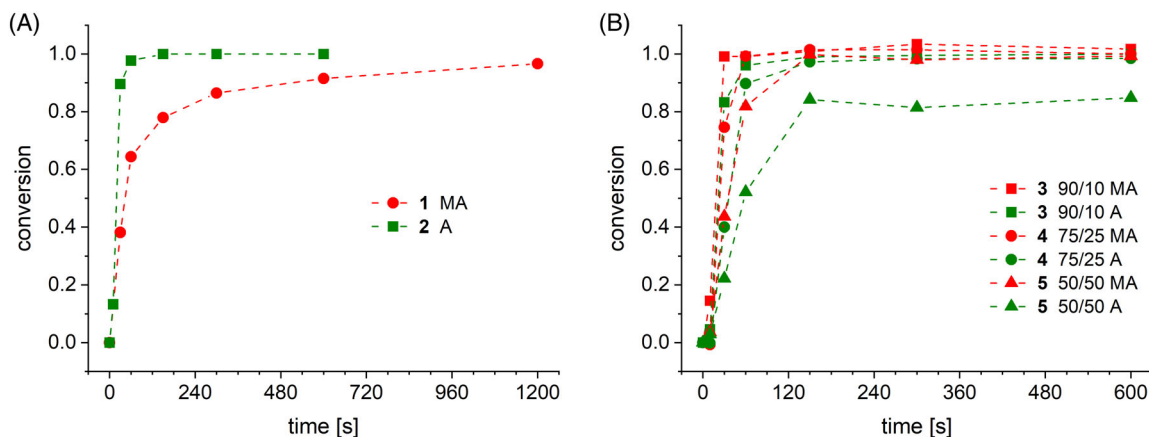

SCHEME 2 Schematic representation of the UV-initiated polymerization in the presence of the ionic liquid (IL) and fumed silica

FIGURE 2 Kinetic investigations for the UV-initiated gel polymer electrolyte (GPE) formation (initator: Ivocerin®) via ^{1}H NMR with EMImTFSI used as internal standard for (A) GPEs based on methacrylates or acrylates, and (B) GPEs based on mixtures of both monomer types [Color figure can be viewed at wileyonlinelibrary.com]

(DSC, Figure S3) of free-standing GPEs 1–3 revealed decomposition temperatures (5% weight loss) of 277–328°C, and no glass transition between −70 and 200°C. Consequently, the GPEs were further investigated regarding their ionic conductivity and, subsequently, in all-organic batteries to study their influence on the cell performance.

Cyclic voltammetry measurements of a free-standing GPE in a 3-electrode configuration with Pt as working and counter electrode and Ag as quasi-reference electrode confirmed the electrochemical stability of the GPE in the potential range in which the redox reactions of PTMA and PI occur (ca. 0.8 and −0.4 V vs. Ag, respectively, Figure S4). Formulations 1–4 were then casted and polymerized directly on the surface of the PTMA cathode (Figure S5), resulting in films with thicknesses between 330 and 380 μm. The anode was added without an additional separator and the cells were galvanostatically charged and discharged. When comparing the cells containing GPEs based on just A or MA monomers (1 and 2), those with the A-based GPEs show higher specific discharge capacities at 0.1C (67 mAh/g compared to 55 mAh/g) and a better cycling stability (63% of the initial capacity at 1C after the 250th cycles, compared to 52% for MA-based GPEs) (Figure 3). At higher rates of 1C and 5C the capacities are similar (1C: 48 mAh/g for both, 5C: 21 mAh/g (A) and 19 mAh/g (MA)). However, the best performance was achieved when a mixture of A and MA with a molar ratio of A/MA of 90/10 was used. The cells showed initial specific capacities of 70 mAh/g at 0.1C, 52 mAh/g at 1C, and 23 mAh/g at 5C, maintaining 62% of the initial capacity after 250 cycles. When the amount of MA was further increased to 25% the cells revealed a significant decrease of the capacity at 5C.
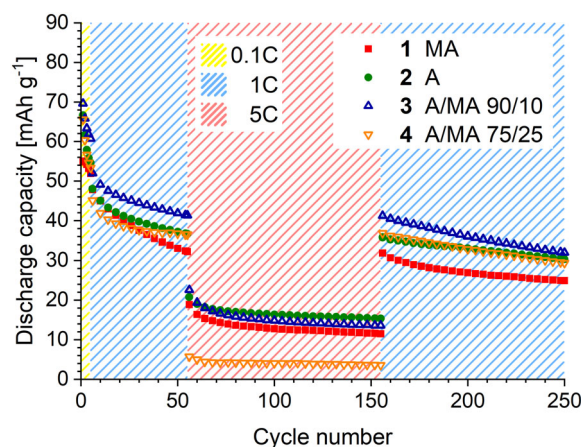

FIGURE 3 Discharge capacities during galvanostatic charge/discharge experiments of coin cells with PTMA cathode, poly(imide) (PI) anode, and gel polymer electrolyte (GPE) (vol$_{IL}$/vol$_M$ 2/1) casted and UV-cured on PTMA electrode with different mixtures of acrylates and methacrylates (5 cycles at 0.1C, 50 cycles at 1C, 100 cycles at 5C, 95 cycles at 1C). For clarity, only every fifth cycle is shown for the 1C and 5C rates [Color figure can be viewed at wileyonlinelibrary.com]

The capacity fading during cycling displays the typical behavior of organic electrode materials, which can be caused by structural and morphological changes due to the intercalation of counter ions during charge/discharge.[29–30] Regarding the Coulombic efficiencies, no effect of the different composition was observed in all cases (Figure S6).

A possible explanation for the different performances of the GPE compositions might be different ionic conductivities. The room temperature ionic conductivities of the formulations were determined by impedance spectroscopy of free-standing GPE-films, which were polymerized between two layers of siliconized PET-foil. The GPEs

based only on As (1) and those containing 10 and 25 mol% MAs (3 and 4) revealed similar high specific ionic conductivities between 2.6 and 2.9 mS/cm, which are within the estimated deviation range of this method (see Figure S7 for exemplary impedance spectrum of GPE 3). The lowest specific conductivity of 2.2 mS/cm was observed for the MA-based GPE (2). This difference in ionic conductivity between the GPEs may not only be an effect of the different monomer-types but of the increased amount of cross-linker that was required for MA-based films to achieve a sufficient mechanical stability (15 mol% compared to 5 mol% for acrylates), resulting in a denser polymer network, which may limit the ion mobility.

Overall, the determined conductivity values are in a very similar range which cannot explain the differences in the cell performances. On the contrary, a comparison with the results of the neat EMImTFSI, which has a significantly higher conductivity (6.6 mS/cm, supplier information), reveals an equal or even slightly increased performance of the GPE-based cells, despite the reduced ion mobility. Therefore, we conclude that the ionic conductivity of the electrolyte is not the limiting factor for the cell performance when values in the same order of magnitude as the neat IL are maintained. In consequence, the composition of the electrolyte appears to be of greater importance. The cell tests prove that the choice of the applied monomers influences the cell performance, even though they are not directly involved in the redox-process. We assume that this effect is induced by a different swelling behavior of the electrode material in the presence of As or MAs, which has an effect on the accessibility for the counter ions to the redox-active sites.

3.3 | Influence of the IL content on the cell performance

To gain a better understanding of the impact of the GPE composition on the cell performance we further analyzed lower ratios of IL to monomer. A first hint is already given by the comparison of the cells containing GPEs and those with pure ILs, where the first displayed higher capacities especially at 1C. To corroborate this trend, GPEs with different IL concentrations, that is, different volumetric M/IL ratios from 2/1 to 1/4, were tested using the best performing composition 3 (A/MA 90/10). The increased monomer concentration has no significant impact on the polymerization rates (Figure S8). However, the specific conductivity of the respective films is significantly affected when the IL content is changed (Figure 4(A)). From an initial value of 2.6 mS/cm at vol_{IL}/vol_M 2/1, the conductivity decreases to 1.1 mS/cm at a ratio of 1/1, 0.26 mS/cm at 1/2, and even to 0.074 mS/cm at 1/4.

Subsequently, charge/discharge experiments in coin cells were conducted to assess whether the lower ionic conductivities of the films affect the cell performance. Against our expectations, a lower ratio of vol_{IL}/vol_M 1/1 leads to a significant increase in discharge capacities of up to 78 mAh/g at 0.1C, 54 mAh/g at 1C and 33 mAh/g even at 5C (Figure 4(B)). Only when the ratio is further reduced to vol_{IL}/vol_M 1/2, the capacities of the cells decreases below the initial values at a ratio IL/M of 2/1. A
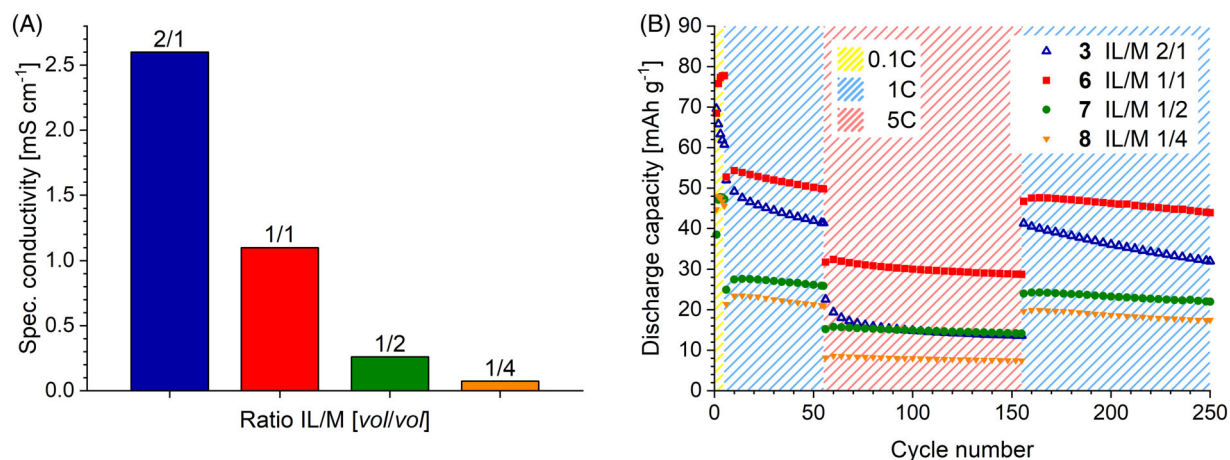

FIGURE 4 (A) Specific conductivities of gel polymer electrolytes (GPEs) with varied ionic liquid (IL) contents. (B) Discharge capacities during galvanostatic charge/discharge experiments of coin cells with PTMA cathode, poly(imide) (PI) anode, and GPE (A/MA 90/10) casted and UV-cured on PTMA electrode with different amounts of EMImTFSI (5 cycles at 0.1C, 50 cycles at 1C, 100 cycles at 5C, 95 cycles at 1C). For clarity, only every fifth cycle is shown for the 1C and 5C rates [Color figure can be viewed at wileyonlinelibrary.com]

correlating effect can be observed in the voltage profiles of the charge/discharge experiments (Figure S9). The difference between charge and discharge voltages slightly decreases at vol_{IL}/vol_M 1/1 compared to 2/1. At a ratio of 1/2, the Ohmic drop significantly increases again. Furthermore, the capacity retention benefits from a lower IL contents. While a cell with vol_{IL}/vol_M 2/1 maintains 62% of its initial capacity at 1C after the 250th cycle, those with 1/1 and 1/2 retain 83% and 88%, respectively.

These results demonstrate that the ionic conductivity of the electrolyte represents the limiting factor for the electrochemical performance of the reported cells only if the values are below a certain threshold (1 mS/cm). For higher conductivities, the interaction between electrolyte and active material gains importance. In particular at high charge/discharge rates, a too high amount of IL impedes the accessibility of the redox sites for the counter ions. However, it can be assumed that the less polar monomers lead to an enhanced swelling of the active electrode materials and, thus, form diffusion pathways for the electrolyte ions, which are maintained after polymerization. Therefore, the compounds forming the polymer matrix play an unexpected but important role in mediation at the electrolyte/composite-interface.

4 | CONCLUSION

The development of solid-state all-organic battery systems depends crucially on the mutual adjustment of the applied components, in particular the electrodes and the GPEs. It bears the opportunity for simplified processing and enhancement of the electrochemical performance toward the theoretical capabilities of the system. The herein conducted adaptations of an IL-based GPE and the organic electrodes revealed several key findings for an optimization of all-organic batteries. Complete conversions within seconds were successfully achieved in UV-initiated polymerization by the application of acrylate instead of methacrylate monomers. The fast polymerization kinetics of the acrylates enabled rapid film formations in less than 1 min even in mixtures containing up to 25 mol% methacrylates. This is a decisive factor for printing processes in particular with regard to mass production. Impedance spectroscopy revealed high ionic conductivities of the resulting films of up to 2.9 mS/cm, which are in the same order of magnitude as the pure IL. Subsequent cycling experiments in all-organic cells with PTMA cathodes and PI anodes confirmed previous observations that cells with GPEs reach higher capacities compared to those with pure IL as electrolyte. Moreover, the variation of the composition of the GPEs surprisingly revealed that the specific capacity increased with a reduced IL/M ratio of 1/1, although the specific ionic conductivity decreased. However, a further decrease of IL content resulted in a drop of performance, which is most likely related to the significantly lower ion content and mobility. These results emphasize that, in addition to a sufficient ion conductivity, the interaction between electrolyte and electrode is a key factor for optimized cell performance. A higher ratio of less polar monomers improves the interaction between the electrode material and the GPE and, thus, the accessibility of the redox-active sites for the electrolyte ions. The results of this work provide new insights for future strategies to enhance the performance of all-organic batteries and, at the same time, increase the opportunities for a production on large scale.

ORCID

Simon Muench https://orcid.org/0000-0003-3710-4682
Ulrich S. Schubert https://orcid.org/0000-0003-4978-4670

REFERENCES

[1] Y. Liang, C.-Z. Zhao, H. Yuan, Y. Chen, W. Zhang, J.-Q. Huang, D. Yu, Y. Liu, M.-M. Titirici, Y.-L. Chueh, H. Yu, Q. Zhang, *InfoMat* **2019**, *1*, 6.

[2] G. L. Kyriakopoulos, G. Arabatzis, *Renew. Sustain. Energy Rev.* **2016**, *56*, 1044.

[3] J. Winsberg, T. Hagemann, T. Janoschka, M. D. Hager, U. S. Schubert, *Angew. Chem. Int. Ed.* **2017**, *56*, 686.

[4] S. Muench, A. Wild, C. Friebe, B. Häupler, T. Janoschka, U. S. Schubert, *Chem. Rev.* **2016**, *116*, 9438.

[5] Y. Liang, Y. Yao, *Joule* **2018**, *2*, 1690.

[6] T. B. Schon, B. T. McAllister, P.-F. Li, D. S. Seferos, *Chem. Soc. Rev.* **2016**, *45*, 6345.

[7] J.-K. Kim, G. Cheruvally, J.-W. Choi, J.-H. Ahn, D. S. Choi, C. E. Song, *J. Electrochem. Soc.* **2007**, *154*, 839.

[8] J.-K. Kim, A. Matic, J.-H. Ahn, P. Jacobsson, *RSC Adv.* **2012**, *2*, 9795.

[9] T. Suga, H. Konishi, H. Nishide, *Chem. Commun.* **2007**, 1730.

[10] K. Nakahara, J. Iriyama, S. Iwasa, M. Suguro, M. Satoh, E. J. Cairns, *J. Power Sources* **2007**, *165*, 398.

[11] W. Huang, Z. Zhu, L. Wang, S. Wang, H. Li, Z. Tao, J. Shi, L. Guan, J. Chen, *Angew. Chem. Int. Ed.* **2013**, *52*, 9162.

[12] Z. Zhu, M. Hong, D. Guo, J. Shi, Z. Tao, J. Chen, *J. Am. Chem. Soc.* **2014**, *136*, 16461.

[13] M. Lécuyer, J. Gaubicher, A.-L. Barrès, F. Dolhem, M. Deschamps, D. Guyomard, P. Poizot, *Electrochem. Commun.* **2015**, *55*, 22.

[14] W. Li, L. Chen, Y. Sun, C. Wang, Y. Wang, Y. Xia, *Solid State Ion.* **2017**, *300*, 114.

[15] S. Muench, R. Burges, A. Lex-Balducci, J. C. Brendel, M. Jäger, C. Friebe, A. Wild, U. S. Schubert, *Energy Storage Mater.* **2020**, *25*, 750.

[16] Press release: Evonik Industries AG, 19 March 2019: Batteries from the printer; https://corporate.evonik.com/Downloads/Corporate/PMs/03_2019/20190318%20Batteries%20from%20the%20printer.pdf (accessed: September **2020**).

[17] www.taettooz.com (accessed: September **2020**).

[18] Press release: Evonik Industries AG, 26 May 2020: Evonik and Ynvisible introduce technology demonstrator for printed electronics; https://corporate.evonik.com/Downloads/Corporate/PMs/05_2020/20200526%20PR%20Evonik%20and%20Ynvisible%20introduce%20technology%20demonstrator.pdf (accessed: September **2020**).

[19] K. Nakahara, S. Iwasa, M. Satoh, Y. Morioka, J. Iriyama, M. Suguro, E. Hasegawa, *Chem. Phys. Lett.* **2002**, *359*, 351.

[20] B. Häupler, A. Wild, U. S. Schubert, *Adv. Energy Mater.* **2015**, *5*, 1402034.

[21] A. Wild, V. Bakumov, M. Korell, EP 3 588 634 A1, **2020**.

[22] A. Manuel Stephan, K. S. Nahm, *Polymer* **2006**, *47*, 5952.

[23] S. H. Chung, Y. Wang, L. Persi, F. Croce, S. G. Greenbaum, B. Scrosati, E. Plichta, *J. Power Sources* **2001**, *97-98*, 644.

[24] P. Raghavan, X. Zhao, J.-K. Kim, J. Manuel, G. S. Chauhan, J.-H. Ahn, C. Nah, *Electrochim. Acta* **2008**, *54*, 228.

[25] M. Wachtler, D. Ostrovskii, P. Jacobsson, B. Scrosati, *Electrochim. Acta* **2004**, *50*, 357.

[26] A. Wild, M. Korell, S. Münch, A. Lex-Balducci, J. Brendel, U. S. Schubert, WO 2020/126200 A1, **2020**.

[27] G. V. R. Reddy, R. Ranganathan, S. Sivakumar, R. Sriram, *Des. Monomers Polym.* **2002**, *5*, 97.

[28] S. G. Roos, A. H. E. Müller, K. Matyjaszewski, *Macromolecules* **1999**, *32*, 8331.

[29] T. Tomai, H. Hyodo, D. Komatsu, I. Honma, *J. Phys. Chem. C* **2018**, *122*, 2461.

[30] H. Kim, D.-H. Seo, G. Yoon, W. A. Goddard, Y. S. Lee, W.-S. Yoon, K. Kang, *J. Phys. Chem. Lett.* **2014**, *5*, 3086.

SUPPORTING INFORMATION

Additional supporting information may be found online in the Supporting Information section at the end of this article.